remote sensing

MDPI

Technical Note

Performance Assessment of Multi-GNSS Real-Time Products from Various Analysis Centers

Chao Yu [1,2], Yize Zhang [1], Junping Chen [1,2,*], Qian Chen [3], Kexin Xu [1,2] and Bin Wang [1]

[1] Shanghai Astronomical Observatory, Chinese Academy of Sciences, Shanghai 200030, China
[2] School of Astronomy and Space Science, University of Chinese Academy of Sciences, Beijing 100049, China
[3] DFH Satellite Co., Ltd., Beijing 100094, China
* Correspondence: junping@shao.ac.cn

Abstract: The performance of real-time precise point positioning (PPP) relies primarily on the availability and quality of orbit and clock corrections. In this research, we collected data streams from 12 real-time mount points of IGS Real-Time Service (RTS) or analysis centers for a one-month period and conducted a performance assessment, including product latency and data availability, accuracy of orbit, clock and positioning performance. The epoch availability of GPS, GLONASS, Galileo and BDS was more than 98.5%, 95.79%, 94.20% and 85.9%, respectively. In addition, the orbit and clock errors of different real-time corrections was investigated. Then, PPP in static and kinematic for 16 IGS stations was conducted. The results show the real-time PPP for different products has a longer convergence time and a slightly worse accuracy than those of the post-processing PPP. For static PPP over 24 h, the real-time products of WHU had the best performance, with a mean RMSE of 1.0 cm in the horizontal and vertical directions and a median convergence time of 12.0 min. The products of CAS had the faster convergence speed due to the shortest product latency. Regarding real-time kinematic PPP for GPS only in an hourly batch, the real-time products of WHU and ESA performed best with a mean RMSE of 10.8 cm and 9.5 cm in the horizontal and vertical directions, respectively. Additionally, the PPP for different real-time products with the multi-GNSS combination obtained higher accuracy than those with GPS only in post-processing or real-time mode, and the PPP with the GPS/GLONASS/Galileo/BDS combination had the fastest convergence speed and best positioning performance. The hourly based kinematic PPP results of CAS, DLR, GFZ and WHU with the GREC combination had positioning errors smaller than 5.2 cm.

Keywords: PPP; SSR corrections; multi-GNSS; real-time positioning

Citation: Yu, C.; Zhang, Y.; Chen, J.; Chen, Q.; Xu, K.; Wang, B. Performance Assessment of Multi-GNSS Real-Time Products from Various Analysis Centers. *Remote Sens.* **2023**, *15*, 140. https://doi.org/10.3390/rs15010140

Academic Editors: Rui Tu, Wei Qu, Kejie Chen and Andrzej Stateczny

Received: 4 December 2022
Revised: 21 December 2022
Accepted: 23 December 2022
Published: 27 December 2022

1. Introduction

Precise Point Positioning (PPP) is a widely used technology and can achieve centimeter-level or even millimeter-level positioning accuracy for a receiver anywhere in the world by applying precise orbit and clock products from the International GNSS Service (IGS) agency or analysis centers (ACs) [1–5]. In order to satisfy the needs for real-time data processing and application, the IGS Real-Time Work Group (RTWG) was established in 2001, and started the Real-Time Service (RTS) which has officially operated since 2013 [6–9]. The RTS provides orbit and clock corrections for GPS and GLOASS dual-systems based on RTCM (Radio Technical Commission for Maritime Services) and NTRIP (Networked Transport of RTCM via Internet Protocol) [10–13]. In addition, considering the continuous improvement of the GNSS network, IGS started "Multi GNSS Experiment" (MGEX) to integrate tracking and analysis of all satellites navigation systems into IGS activities [14]. With the development of Galileo and BDS, CNES has become the first analysis center with four-system state space representation (SSR) corrections (IGSMAIL-7183). At present, the RTS products include BKG (Bundesamt für Kartographie und Geodäsie), CAS (The Institute of Geodesy and Geophysics (IGG) of the Chinese Academy of Sciences), CNES

(Centre National d'Etudes Spatiales), DLR (Deutsches Zentrum fur Luft-und Raumfahrt), ESA (European Space Agency), GFZ (Deutsches GeoForschungsZentrum) [15], GMV (GMV Aerospace and Defense), NRC (Natural Resources Canada), WHU (Wuhan University) and the combined IGS products [16]. Regarding the combined IGS products, two different strategies are used for combining three IGS RTS products, i.e., IGS01, IGS02 and IGS03. IGS01 is single-epoch combination solution [7,8]. IGS02 and IGS03 are Kalman Filter combination solutions [8,17]. Specifically, IGS01 supports only the GPS constellation, while IGS02 supports the GPS, GLONASS and Galileo constellations, and IGS03 is an experimental product for the GPS, GLONASS, Galileo and BDS constellations.

Some studies have researched the quality of real-time corrections [8,9,12,13,18–27], but most assessments focus on a single data stream or only GPS constellation. Especially as more analysis centers start to provide BDS-3 satellites corrections, it is necessary to investigate the performance of the multi-GNSS real-time products from various ACs. This research focuses on the comprehensive evaluation of the multi-GNSS real-time products of IGS RTS. In Section 2, the methods of the generation of real-time satellite orbit and clock products from SSR are introduced. Sections 3 and 4 evaluate the data availability, latency and accuracy of real-time products based on one month of data. Section 5 reports on the precise point positioning experiment that aimed to evaluate the convergence and accuracy of positioning performance. The conclusions are summarized in the conclusions section.

2. Methods

2.1. Matching the Issue of Data (IOD)

Real-time RTCM-SSR corrections are aligned to special broadcast ephemeris by using IOD in SSR orbit and clock messages. The IOD value for GPS and Galileo is directly equal to the issue of data ephemeris (IODE) from navigation data [25]. However, for GLONASS and BDS, the IOD is derived from broadcast ephemeris. The IOD for GLONASS is calculated as [28]:

$$IOD_{GLONASS} = \frac{MOD(SoD_{brdc} + 3 \times 3600, 86400)}{900} \quad (1)$$

where SoD_{brdc} is the seconds of day in UTC from the reference time of broadcast ephemeris; the range of $IOD_{GLONASS}$ is between 1~95.

The IOD for BDS is calculated as [28]:

$$IOD_{BDS} = MOD\left(\frac{MOD(TOE_{brdc}, 604800)}{720}, 240\right) \quad (2)$$

where TOE_{brdc} denotes the seconds of week, that is, ephemeris reference time, and the range of IOD_{BDS} is between 0~235.

It is worth noting that the reference time of ephemeris (TOE) parameter of decoded the BDS broadcast may be greater than 604,800 at the beginning of a week, which will lead to a mismatch of IOD between SSR products and broadcast ephemeris. Therefore, the IOD for BDS RTCM-SSR needs to be reprocessed before matching, and we assume the IOD for BDS RTCM-SSR is switched within ten minutes after a new ephemeris is updated. The real-time reprocessing method for the IOD for BDS RTCM-SSR is listed in the following:

$$IOD_{SSR} = \begin{cases} IOD_{SSR} - 120, & 0 < TOE_{SSR} \leq 86400 \; and \; IOD_{SSR} \geq 120 \\ IOD_{SSR} - 120, & 86400 < TOE_{SSR} < 87000 \; and \; IOD_{SSR} \neq 120 \\ IOD_{SSR}, & Otherwise \end{cases} \quad (3)$$

where IOD_{SSR} is the original or reprocessed IOD of BDS SSR products; TOE_{SSR} is the seconds of week of RTCM-SSR corrections. Certainly, IOD_{SSR} is equal to the original value from real-time RTCM-SSR streams when TOE_{SSR} is not within the specific time range.

2.2. Real-Time Orbit and Clock Recovery

The real-time RTCM-SSR corrections can be expressed as:

$$SSR(t_0, IOD) = \left(\delta r, \delta a, \delta c, \delta \dot{r}, \delta \dot{a}\ , \delta \dot{c}\ , A_0, A_1, A_2\right) \tag{4}$$

where t_0 is the reference time obtained from SSR corrections. $(\delta r, \delta a, \delta c)$ are the orbit corrections in radial, along-track, cross-track components, respectively. $(\delta \dot{r}, \delta \dot{a}\ , \delta \dot{c}\ )$ are the velocity of orbit corrections in three components, respectively. (A_0, A_1, A_2) are the polynomial coefficients of clock corrections. Complete orbit correction vector δorb is computed as [28]:

$$\begin{cases} \delta orb = \begin{bmatrix} e_{radial} \\ e_{along} \\ e_{cross} \end{bmatrix} \times \begin{bmatrix} \delta r \\ \delta a \\ \delta c \end{bmatrix} + \begin{bmatrix} e_{radial} \\ e_{along} \\ e_{cross} \end{bmatrix} \times \begin{bmatrix} \delta \dot{r} \\ \delta \dot{a} \\ \delta \dot{c} \end{bmatrix} \times (t - t_0) \\ \begin{bmatrix} e_{radial} \\ e_{along} \\ e_{cross} \end{bmatrix} = \begin{bmatrix} \frac{\dot{r}}{|\dot{r}|} \times \frac{r \times \dot{r}}{|r \times \dot{r}|} \\ \frac{\dot{r}}{|\dot{r}|} \\ \frac{r \times \dot{r}}{|r \times \dot{r}|} \end{bmatrix} \end{cases} \tag{5}$$

where $r, \dot{r}$ are the satellite positions and velocity vector at epoch t calculated by broadcast ephemeris, respectively. (e_{radial}, e_{along} , e_{cross}) are the unit vectors in radial, along-track, and cross-track components, respectively. Finally, the corrected satellite position can be expressed as [28]:

$$X = X_{brdc} + \delta orb \tag{6}$$

where X denotes the satellite positions; X_{brdc} denotes the satellite positions at epoch t calculated by broadcast ephemeris.

Similarly, the satellite clock is corrected as follows [28].

$$\begin{cases} \delta clk = A_0 + A_1(t - t_0) + A_2(t - t_0)^2 \\ Clk = Clk_{brdc} + \frac{\delta clk}{c} \end{cases} \tag{7}$$

where δclk denotes the correction of the satellite clock; Clk is the precise satellite clock used for precise point positioning; Clk_{brdc} is the satellite clock at epoch t_0 calculated by broadcast ephemeris; and c is the speed of light in meter per second in the vacuum.

3. Latency and Availability of SSR Products

Real-time PPP relies on high-precision orbit and clock products. However, apart from the errors of real-time products themselves, the latency of real-time products may introduce additional prediction errors. Furthermore, the data availability of real-time products influences the continuity and stability of RT-PPP solutions. Therefore, the latency and data availability for real-time products was first assessed.

In order to investigate the performance of real-time products, one month of SSR data, from DOY 330 to DOY 360 in 2021, of 12 real-time mount points, including BKG, CAS, CNES, DLR, ESA, GFZ, GMV, NRC, WHU, IGS01, IGS02 and IGS03, were recorded using the BNC software [29]. A description of the RTCM-SSR mount points is presented in Table 1, and the statistical results of latency is given. It should be noted that the latency information may be affected by the network environment of receiving, but the results can be still taken as a reference. The IGS products were combined from individual solutions and the latency was larger than the other products. The mean latencies of IGS01, IGS02 and IGS03 were about 30.70 s, 37.50 s and 37.85 s, respectively. The real-time corrections of CAS had the shortest latency with a mean value of 6.18 s among the various ACs. Except for the corrections of IGS, the largest latency was from GMV with a mean value of 18.89 s. In addition, the SSR products of ESA had the smallest STD of 0.81 s over the data collection period, and the largest STD was from IGS01 with a value of 3.38 s. Other SSR products

such as BKG, GFZ and GMV also had a large STD value. Even though the difference between STD values seems small, it indirectly showed the number of abnormal latency or interruption which will limit the convergence of kinematic positioning.

Table 1. RTCM-SSR mount points Description.

Products	Systems	Update Interval (Orbit/Clock)	Average of Latency/s	STD of Latency/s
BKG	G + R + E	60 s/5 s	16.06	1.65
CAS	G + R + E + C	5 s/5 s	6.18	1.17
CNE	G + R + E + C + J	5 s/5 s	18.89	1.07
DLR	G + R + E + C + J	30 s/5 s	14.03	0.95
ESA	G	5 s/5 s	12.31	0.81
GFZ	G + R + E + C	5 s/5 s	13.40	1.57
GMV	G + R + E	10 s/10 s	13.90	3.14
NRC	G	5 s/5 s	9.19	1.40
WHU	G + R + E + C	5 s/5 s	16.25	1.05
IGS01	G	5 s/5 s	30.70	3.38
IGS02	G + R + E	60 s/10 s	37.50	1.09
IGS03	G + R + E + C	60 s/10 s	37.81	1.00

Figure 1 presents the epoch availability of SSR corrections; availability of orbit and clock corrections is given separately in consideration of the difference in the update interval for some ACs. The unhealthy satellites, which could be obtained from broadcast ephemeris, such as G11, G28, R11, E14 and E18 were excluded during the experiment. The epoch availability of GPS satellites from various ACs was more than 98.5%, and the highest availability of GPS corrections was from ESA and was 99.75%. For GLONASS, the products of WHU had the lowest epoch availability, at 95.79%, while GFZ had the highest epoch availability, at 99.37%. For Galileo, the epoch availability of IGS02 and IGS03 was obviously lower than other real-time products, and IGS02 had the lowest availability, at 94.20%. As for BDS, the epoch availability of DLR, GFZ and WHU was higher than 98.6%. The epoch availability of CAS and CNES were about 95.1% and 91.4%, respectively. However, IGS03 had the lowest epoch availability, at 85.9%, for the BDS constellation, which could have been due to discontinuities or outlier screening. Furthermore, the epoch availability of clock corrections was almost equal to the availability of orbit corrections for most SSR products as opposed to that of CAS, which showed that the clock corrections of Galileo and BDS from CAS may have more outages.

The number of available satellites per epoch for real-time products is given in Figure 2. There is little difference in the number of available GPS and GLONASS satellites among different SSR products, while the number of available GPS satellites was 29 for all real-time products in the test period. For GLONASS, the average number of available satellites from nine real-time products was 19 or 20. The significant inconsistency among real-time corrections is presented for Galileo and BDS. For most real-time corrections, the number of available Galileo was 22, while the SSR corrections from GFZ contain only 18 Galileo satellites. The SSR corrections of CAS, GFZ and WHU contained 42 BDS satellites, while the products of CNES, DLR and IGS03 contained 25, 27 and 17 BDS satellites, respectively. In general, the maturity of observation network determines the continuity and stability of SSR corrections. GPS satellites had the highest data availability for different SSR corrections; the next were GLONASS satellites, and the last were Galileo and BDS satellites.

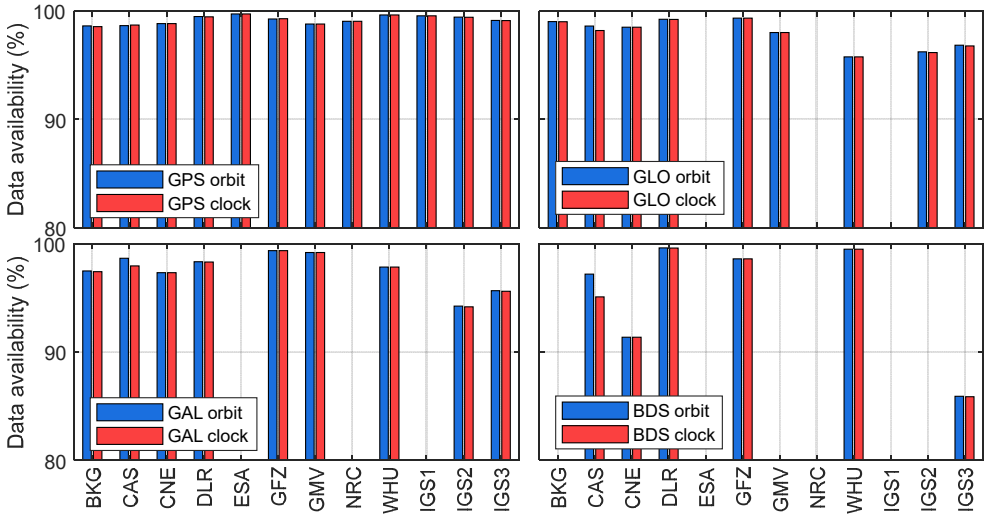

Figure 1. Epoch availability of SSR corrections during the experiment.

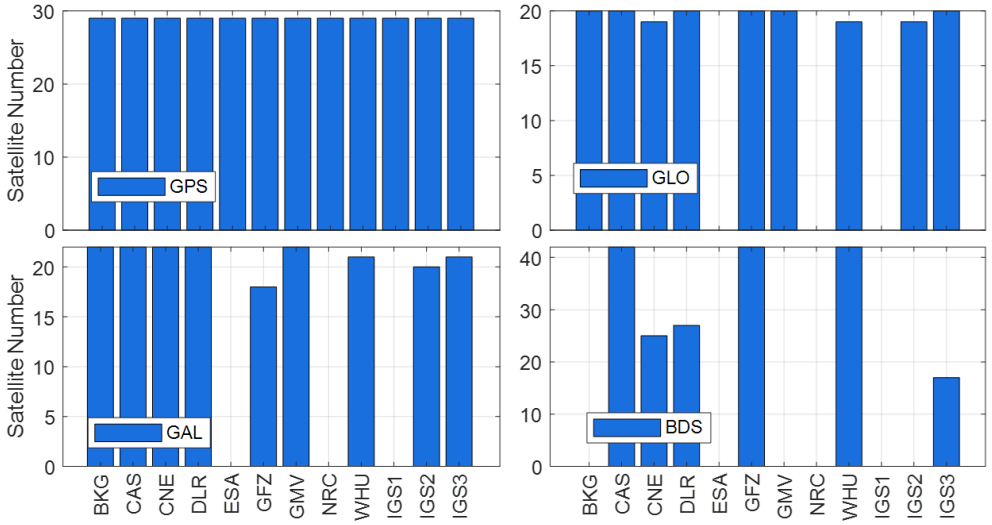

Figure 2. Satellite availability of SSR products.

4. Accuracy Evaluation of SSR Products

Final precise post-processing products for multi-GNSS from Wuhan University with more than 120 satellites have high consistency with the other final multi-GNSS products [30], thus it was chosen as a reference to evaluate the real-time products. Note that most of the SSR products that are referred to the antenna center have been generated by using a primary frequency center convention instead of the ionospheric-free combination according to IGS SSR format [28]. However, the real-time SSR corrections of NRC still adopted the ionospheric-free combination convention during this period. Furthermore, the products of CAS had an interruption in DOY 346 and restarted in DOY 348 with a conversion of the phase center reference from the L1 center convention to the L1/L2 ionospheric free linear combination. Interestingly, we found that the products of CAS switched back to the single frequency center convention from DOY 97, 2022. For clock comparison, the median of clock errors each epoch was removed as the common offset of clock products.

4.1. GPS Orbit and Clock Corrections

Figure 3 presents the accuracy of GPS SSR products. The radial component of all SSR products was generally better than 2.2 cm. The SSR products were better than 7.7 cm in the along-track and 4.0 cm in the cross-track component. IGS01 had the best performance for GPS orbit, i.e., 1.4, 2.8 and 1.9 cm in radial, along-track and cross-track components,

respectively. The STD and RMS of clock errors from 12 SSR products also are shown in Figure 3. The mean STD of the clock errors for all GPS clock products was better than 0.2 ns. The clock corrections of WHU performed the best, with a mean STD of about 0.06 ns, which could be due to better consistency with the reference product. The clock products of CNES, ESA, GMV and IGS01 also achieved similar accuracy, which were better than 0.1 ns.

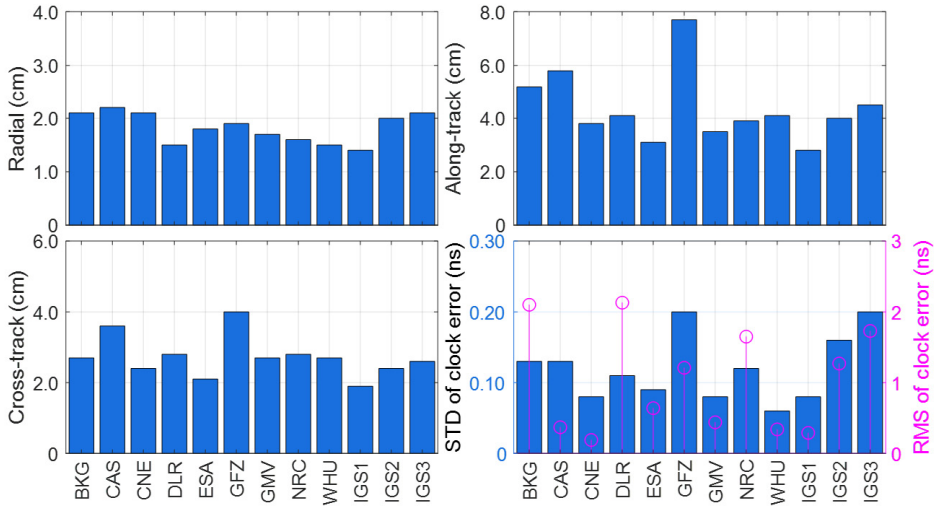

Figure 3. The accuracy of GPS SSR products. The STD (Left y axis and blue) and RMS (Right y axis and magenta) of clock errors is presented in the lower-right subplot.

4.2. GLONASS Orbit and Clock Corrections

Nine mount points provide GLONASS SSR corrections, and Figure 4 shows the accuracy of GLONASS SSR products. The RMS of different GLONASS orbit errors ranged from 3.1 cm to 5.2 cm in the radial, and the products of CNES had the best performance. The accuracy in the other orbit directions of all GLONASS orbit products were at the same level, with an RMS value of about 6.0 cm in the cross-track and 10.0 cm in the along-track direction. For clock comparison, except for that of GMV, the STD of GLONASS clock corrections for different real-time SSR products ranged from 0.20 ns to 0.58 ns. The GLONASS clock corrections of CNES had the best performance, with a mean STD of 0.2 ns. The clock errors of IGS02 and IGS03 had a mean STD of about 0.58 ns, while the worst result was that of GMV with a mean STD of 1.77 ns.

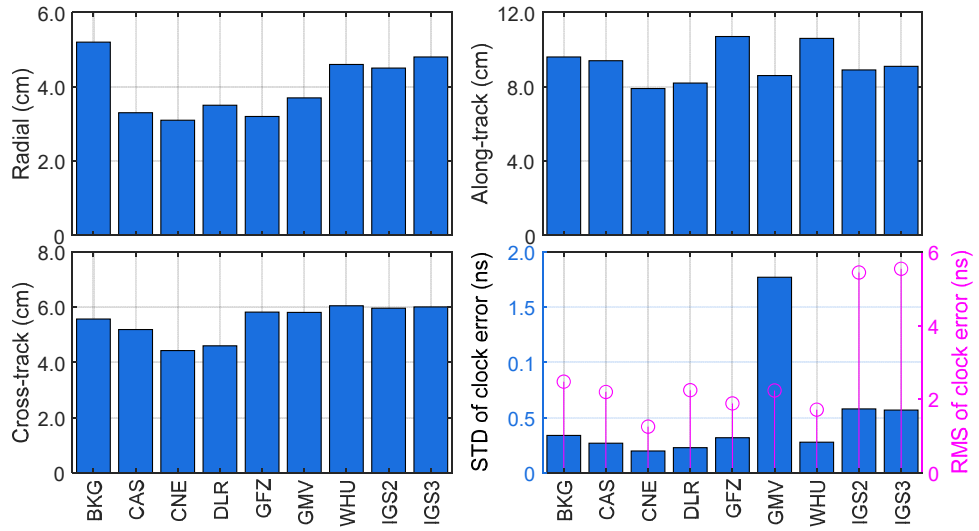

Figure 4. The accuracy of GLONASS SSR products. The STD (Left y axis and blue) and RMS (Right y axis and magenta) of clock errors is presented in the lower-right subplot.

4.3. Galileo Orbit and Clock Corrections

Figure 5 shows the accuracy of Galileo SSR products. It can be seen that the orbit accuracy of Galileo real-time products was a bit worse than those of GPS, but better than those of GLONASS. The Galileo orbit products of WHU were the best, with a mean RMS of about 2.1 cm, 6.6 cm and 3.7 cm in the three directions of orbit, respectively. Overall, the Galileo real-time orbit corrections were better than 3.5 cm, 8.2 cm and 4.6 cm in orbital three directions. The Galileo clock products from all ACs were generally better than those of GPS, which may have been due to the highly accurate hydrogen clocks. The mean STD of different Galileo clock products ranged from 0.10 ns to 0.15 ns, except that of GFZ with a STD of 0.22 ns.

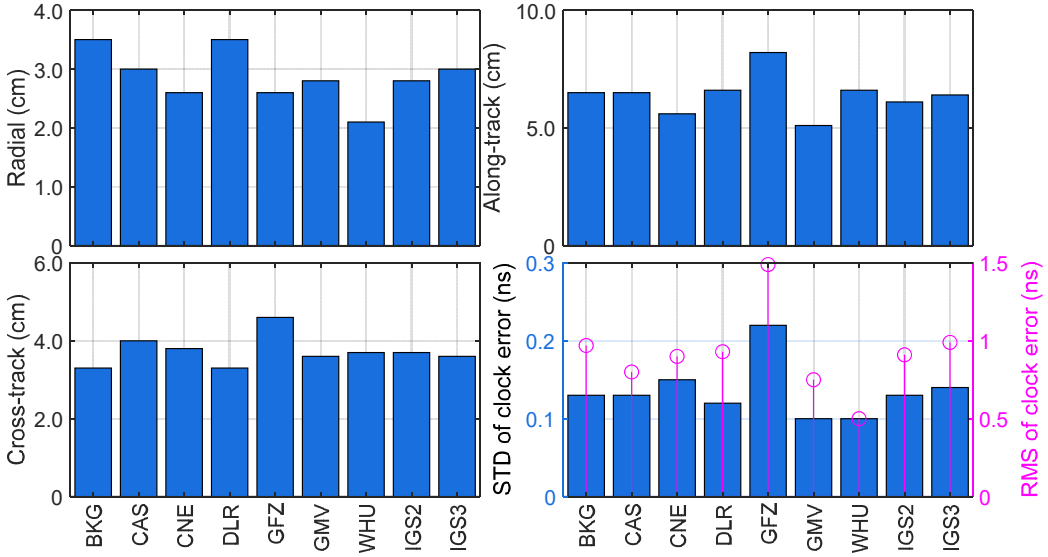

Figure 5. The accuracy of Galileo SSR products. The STD (Left y axis and blue) and RMS (Right y axis and magenta) of clock errors is presented in the lower-right subplot.

4.4. BDS Orbit and Clock Corrections

Furthermore, six SSR corrections, including CAS, CNES, DLR, GFZ, WHU and IGS03, contained BDS satellites and were assessed. It should be noted that the SSR corrections of CAS, CNES, GFZ, WHU and IGS03 provide all BDS satellites, including GEO, IGSO and MEO satellites. However, the products from DLR provide only 27 MEO satellites for BDS. In order to analyze the BDS SSR corrections, the errors of BDS-3 for IGSO and MEO are separately shown in Figure 6. The errors of the BDS products were significantly larger than GPS. The mean RMS of real-time products from DLR for MEO satellites had the best performance with 3.9 cm, 9.5 cm and 4.3 cm in the radial, along-track and cross-track components, respectively. Likely, the clock corrections of DLR for the MEO satellites had the best accuracy with a mean STD of 0.17 ns and an RMS of 0.39 ns. Furthermore, the accuracy of BDS IGSO (from C38 to C40) products was worse than that of MEO. Abnormal orbit and clock errors could be found for the IGSO products of GFZ in the period that may be in testing. The best accuracy of BDS SSR products for IGSO was from WHU with a mean RMS of about 10 cm, 16.6 cm and 11.7 cm in the three components, respectively. The mean STD of clock products from WHU was 0.42 ns, but with a slightly larger RMS value of 1.96 ns. IGS03 had the second-best performance for IGSO satellites with a mean STD of 0.42 ns and an RMS of 1.16 ns. The mean STD for IGSO clock products of CAS and CNES was about 0.66 ns. However, the products of GFZ had the largest clock errors among the six real-time products, with a mean STD of 2.98 ns.

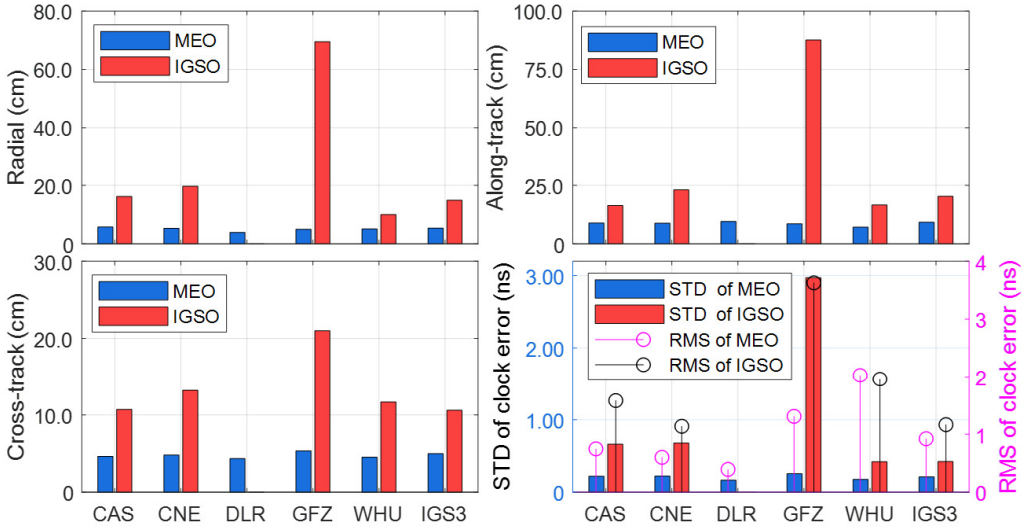

Figure 6. The accuracy of BDS SSR products. The STD (Left y axis and blue for MEO, red for IGSO) and RMS (Right y axis and magenta for MEO, black for IGSO) of clock errors is presented in the lower-right subplot.

5. PPP Validation

5.1. Date Set

In this section, 16 globally distributed IGS stations, which received observations from at least four systems, were selected for PPP validation from DOY 330 to DOY 360 in 2021. The distribution and name of these stations are presented as Figure 7. Two modes were designed to determine the difference between post-processing mode and real-time mode. The difference between post-processing mode and real-time mode was whether data latency was considered. The software Net_Diff was extended and used to verify post-processing and real-time precise positioning with the SSR corrections [31,32]. The positioning strategies are presented in Table 2.

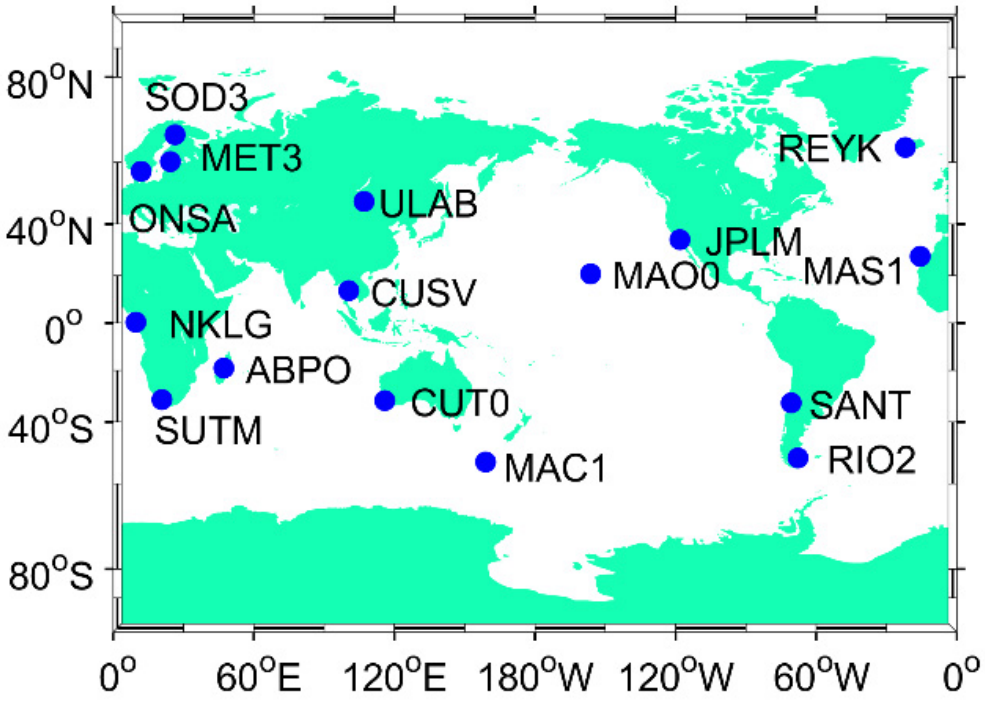

Figure 7. Sixteen globally distributed IGS stations for PPP validation.

Table 2. The positioning strategies of PPP.

Parameter	Strategies
Solution	Static/kinematic
Sampling rate	30 s
Cut-off elevation	10°
Frequency selection	GPS: L1/L2; GLONASS: G1/G2; GALILEO: E1/E5a; BDS: B1I/B3I
Estimator	Kalman filter
Cycle slip	Detected by MW and GF
Ionospheric delay	Eliminated by ionosphere-free combination
Orbit and clock product	Real-time broadcast ephemeris + SSR corrections
Receiver clock	Estimated as white noise process
Weighing strategy	Elevation-dependent weighing model, 3 mm and 0.3 m for phase and code, respectively
Phase ambiguities	Float
antenna phase center	igs14.atx
Tropospheric delay	Corrected (GPT2w + SAAS + VMF [33]) + estimated as a random-walk noise process
Receiver ISB	Estimated system bias as random-walk noise process [34]
Station reference coordinates	IGS weekly SINEX solutions
System combined	G/GRE/GREC

5.2. Static Precise Point Positioning

Convergence time is an important indicator for evaluating precise point positioning. The convergence time for different combinations and SSR products was counted and is shown as boxplots in Figure 8. In these boxplots, the central mark represents the median, and the bottom and top edges of the box represent the 25th and 75th percentiles, respectively. Outliers are plotted individually using the plus symbol [35]. For each daily (24-h) PPP solution, the position was considered to have converged when the position errors stayed within 20 cm for ten consecutive epochs.

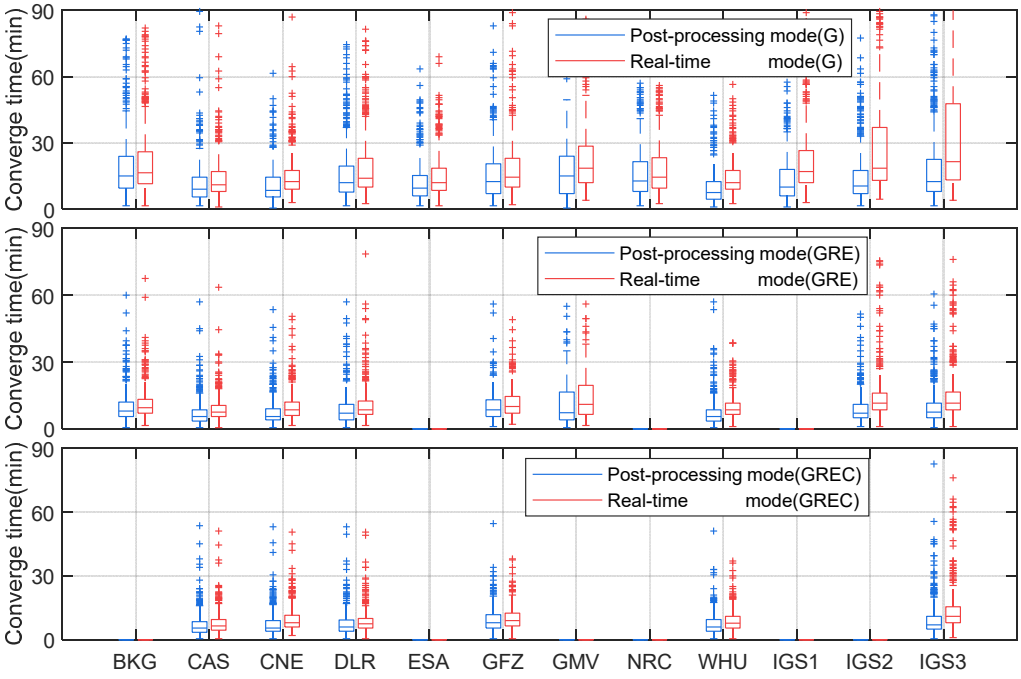

Figure 8. The convergence time of static PPP using different SSR products for 16 IGS stations.

For the post-processing mode, the products of WHU had the shortest mean convergence time for GPS only with a median of 7.5 min, while the products of BKG had the

longest convergence time with a median of 15.0 min. The results were directly related to data availability and the accuracy of GPS corrections. In real-time mode, the products of CAS had the shortest convergence time for GPS only with a median of 11.0 min, while the products of IGS03 had the longest convergence time with a median of 21.5 min. Obviously, the real-time mode requires a longer convergence time than the post-processing mode for different real-time corrections, mainly due to the extrapolation errors of orbit or clock corrections from SSR latency. Compared to the post-processing mode, the degradation of convergence time for different corrections in real-time mode was about 10.0% to 76.2%. Specifically, IGS03, the real-time products with the longest latency, had the worst convergence speed with a degradation of convergence time from a median of 12.5 min in the post-processing mode to 21.5 min in the real-time mode. The degradation of convergence speed in real-time mode for CAS which had the shortest latency was about 22.2%, and a median of convergence time was from 9.0 min in post-processing mode to 11.0 min in real-time mode. Apart from the results from the combined solutions of IGS, the products of GMV had the slowest convergence speed with a median of 18.5 min in real-time mode.

Furthermore, the convergence speed of the GPS/GLONASS/Galileo (GRE) combination for the two modes was significantly faster than that of GPS only, which mainly benefited from the increased number of satellites especially for Galileo satellites. The median convergence time of the GRE combination ranged from 5.5 min to 8.5 min in post-processing mode for different real-time products, while it ranged from 7.5 min to 11.5 min in real-time mode. Compared to the results with GPS only, the convergence time with the GRE combination for different real-time products reduced by 26.7~51.7% in post-processing mode and reduced by 29.2~46.5% in real-time mode. In addition, the results with the GRE combination for those SSR products which were unstable or had large latency had a more positive effect on the convergence speed, such as the results of IGS03 had the largest improvement in convergence speed with 46.5% in real-time mode. The smallest improvement was those of WHU with a value of 29.2% in real-time mode. As for the GPS/GLONASS/Galileo/BDS (GREC) combination, the convergence speed showed a small improvement over the results of the GRE combination, and the improvement for different real-time products was not more than 14.3%. In some ways, the little improvement was limited by the continuity of BDS corrections. Therefore, the real-time services may need to pay more attention to the satellite model and continuity of BDS corrections to ensure the multi-GNSS real-time applications in the future. Moreover, compared to the GRE combination, the abnormal results of the GREC combination were obviously reduced.

Figure 9 presents the positioning accuracy of static PPP for different SSR products. The positioning errors for static PPP in real-time mode are slightly larger than in post-processing mode. The positioning accuracy of GMV in real-time mode was worse than in post-processing mode, which was mainly because the instability of GMV SSR corrections. On the whole, the results of static PPP in real-time mode with GPS only for all SSR products had an accuracy of better than 3.2 cm in the horizontal and 2.5 cm in the vertical directions, respectively. The best performance results were from WHU with a mean RMS of 1 cm in the horizontal and vertical directions. Moreover, for the three real-time products of IGS, IGS01 had the best positioning accuracy with a mean RMS of 2.1 cm in the horizontal and 1.8 cm in the vertical directions. The positioning for static PPP with the GRE and GREC combination could obtain higher accuracy than GPS only, but not more than 17.1%. Furthermore, the positioning accuracy of the GRE or GREC combination was better than 3.5 cm in three-dimensional position. The results of the GRE or GREC combination from the WHU real-time products had the highest positioning accuracy with 0.9 cm and 1.1 cm in the horizontal and vertical directions, respectively.

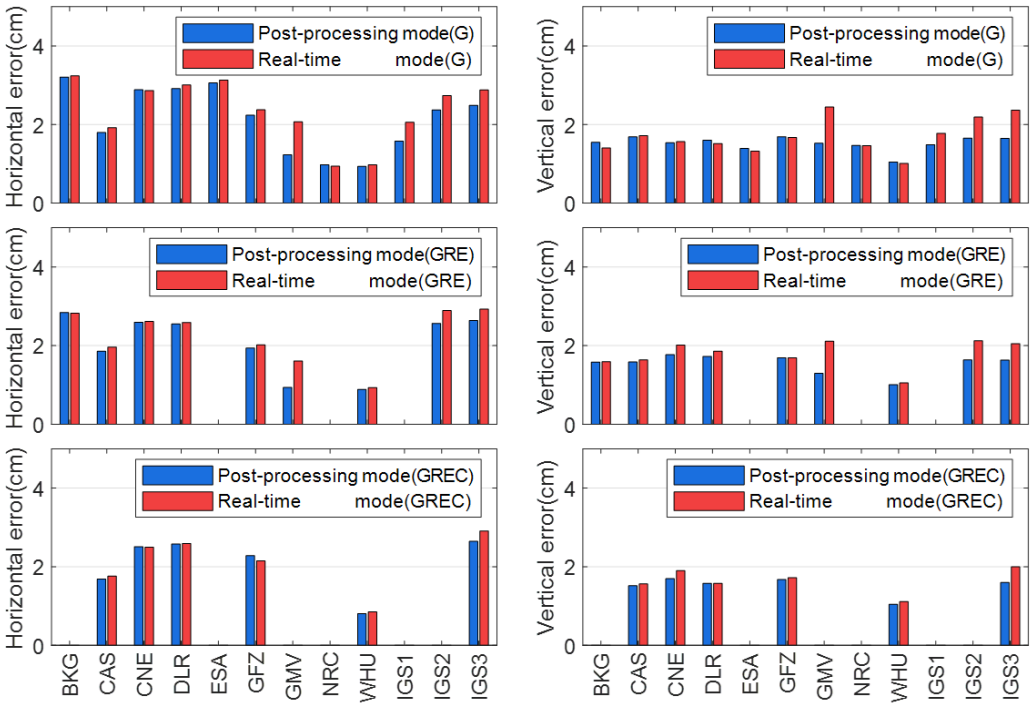

Figure 9. Static PPP errors using different SSR products for 16 IGS stations (24h).

5.3. Simulated Kinematic Precise Point Positioning

For kinematic PPP, the convergence time of the different SSR corrections and combinations is shown in Figure 10. The position was considered to have converged when the position errors stayed within 15 cm in the horizontal and 25 cm in the vertical direction for 10 consecutive epochs.

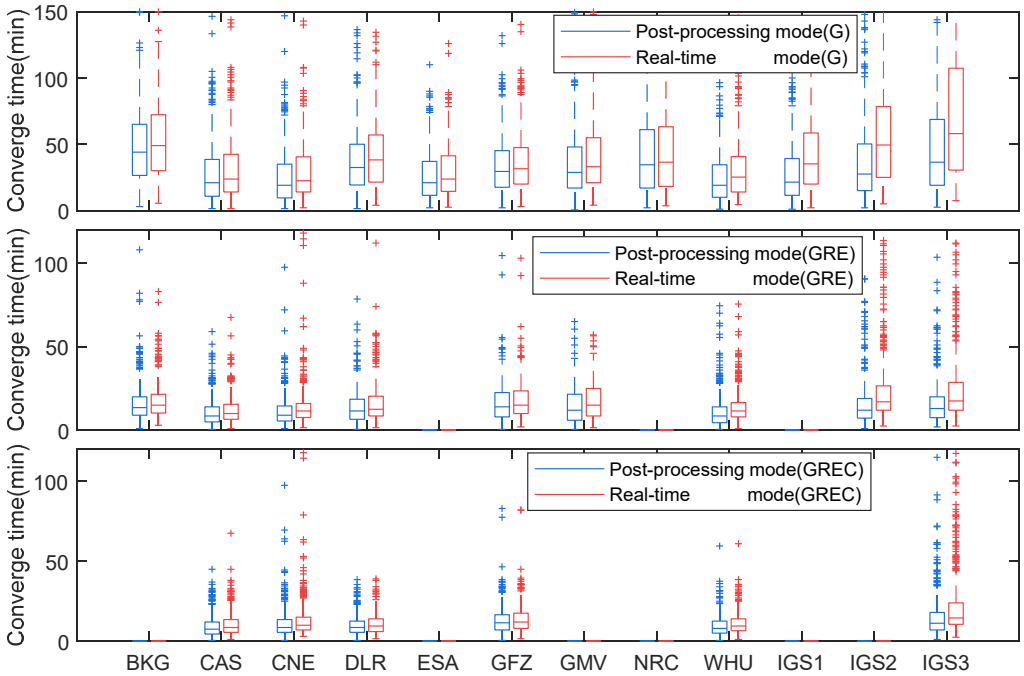

Figure 10. The convergence time of kinematic PPP using different SSR products for 16 IGS stations.

The median convergence time of kinematic PPP in post-processing mode with GPS only for different real-time products ranged from 19.0 min to 44.0 min, while it ranged from 22.5 min to 58.0 min in real-time mode. The large latency had a more negative effect on

the convergence speed for kinematic PPP. The degradation of the convergence time in real-time mode for the SSR products of IGS01, IGS02 and IGS03 was 64.0%, 80.0% and 58.9%, respectively. However, the degradation of the median convergence time for other SSRs was not more than 32.9%, and the degradation of convergence speed for CAS was 13.1%. In real-time mode, CNES had the fastest convergence speed with a median convergence time of 22.5 min for kinematic PPP with GPS only, and the second best was that of CAS and ESA with a value of 23.75 min. Furthermore, the convergence speed of kinematic PPP with the multi-GNSS combination was faster. Compared to the kinematic PPP with GPS only, the improvement in convergence time for different real-time products with the GRE combination ranged from 48.9% to 69.8%. The median convergence time for different real-time products with the GRE combination ranged from 10.0 min to 17.5 min. The products of CAS for kinematic PPP with the GRE combination had the shortest convergence time; the second was from CNES and WHU with a value of 11.5 min. The products of IGS03 had the longest convergence time with a value of 17.5 min. By adding BDS satellites, the convergence speed for kinematic PPP was further improved. The median convergence time for the six real-time products ranged from 8.5 min to 14.5 min. Low latency on the convergence speed of kinematic positioning was still decided an advantage under the condition of equal-precision real-time corrections. The products of CAS still had the fastest convergence speed with a median of 8.5 min, while the products of DLR and WHU which had the higher accuracy of orbit and clock had the second fastest convergence speed with a median of 9.5 min.

Figure 11 presents the RMS of kinematic PPP errors on an hour scale for 16 globally distributed IGS stations using different real-time products; the positioning accuracy was set as the last 10 epochs for each hourly PPP solution. For GPS-only, the results of ESA and WHU products had the best performance for kinematic PPP on an hour scale with a mean RMS of 10.8 cm in the horizontal and 9.5 cm in the vertical direction in real-time mode. The results of CAS, CNES were slightly worse than those of WHU. The results of IGS03 had the worst performance with a mean RMS of 19.0 cm in the horizontal and 17.4 cm in the vertical direction in real-time mode.

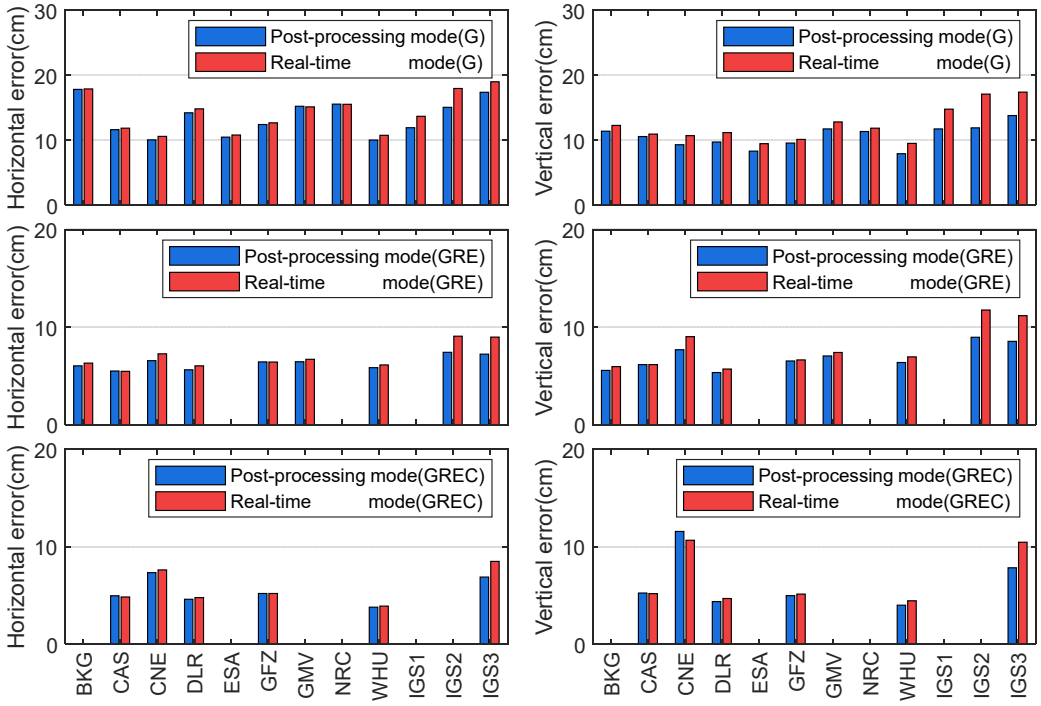

Figure 11. Simulated kinematic PPP errors using different SSR products for the 16 IGS stations (1h).

In contrast to the results of static PPP, the results of kinematic PPP with the multi-GNSS combination showed increased improvement for the positioning accuracy. Compared with the results of GPS only, the improvement of accuracy for different real-time products with the GRE combination ranged from 23.0% to 60.0%. The results with the GRE combination of DLR performed the best with a mean RMS of about 6.0 cm in the horizontal and 5.7 cm in the vertical direction in real-time mode, while IGS02 has the worst performance with a mean RMS of 9.1 cm and 11.8 cm in the horizontal and vertical directions, respectively. Moreover, the improvement of positioning accuracy for kinematic PPP with the combination of GREC for kinematic PPP in real-time mode ranged from 49.4% to 72.8% compared to those with GPS only. The results of CAS, DLR, GFZ and WHU for kinematic PPP in an hour scale with the GREC combination had positioning errors of better than 5.2 cm. Furthermore, the results of CNES and IGS03 had larger positioning errors because of the poor continuity of BDS corrections with the positioning errors of 7.6 cm and 8.5 cm, respectively.

6. Conclusions

Real-time services provide orbit and clock corrections with multi-GNSS satellites to support real-time applications. We performed a comprehensive evaluation of the multi-GNSS real-time products of IGS RTS based on a one-month data stream from 12 mount points.

For the product's latency information, the real-time SSR products of CAS had the smallest latency with an average of 6.18 s. The real-time products of IGS, which were combined by individual solutions, had the largest latency with averages of 30.7 s, 37.5 s and 37.8 s for those of IGS01, IGS02 and IGS03, respectively. The average latency of other SSR products ranged from 9.18 s to 18.89 s. The epoch availability of all SSR corrections was more than 98.6%, 95.8%, 94.2% and 85.9% for GPS, GLONASS, Galileo and BDS, respectively. Furthermore, the number of available satellites per epoch for different SSR products was more than 29, 19 and 18 for GPS, GLONASS and Galileo, respectively. For BDS satellites, the SSR corrections of CAS, GFZ and WHU had available BDS satellites of 42 per epoch, while the products of IGS03 contained the least BDS satellites.

The orbit accuracy of GPS SSR products was better than 2.2 cm, 7.7 cm and 4.0 cm in the radial, along-track and cross-track components, respectively. The mean STD of clock errors for all GPS SSR products was better than 0.2 ns. As for GLONASS, the orbit errors were better than 5.2 cm, 10.7 cm and 6.1 cm in the three components, respectively. The STD of clock errors for nine GLONASS real-time products ranged from 0.2 ns to 1.77 ns; the orbit errors of Galileo real-time products were better than 3.5 cm, 8.2 cm and 4.6 cm in the three directions, respectively. The clock errors for nine Galileo real-time products were better than 0.22 ns. Moreover, only BDS-3 satellites were assessed. The orbit of BDS-3 MEO ranged from 3.9 cm to 5.7 cm in the radial direction, from 7.2 cm to 9.5 cm in the along-track direction and from 4.4 cm to 5.4 cm in the cross-track direction. The errors of the IGSO were larger than those of MEO.

The accuracy of static and kinematic PPP is discussed in post-processing and real-time mode. The results of post-processing mode were directly related to data availability and the accuracy of real-time products. Due to the prediction errors caused by latency, the results of the real-time mode had the longer convergence and slightly worse positioning accuracy than the post-processing mode. For static PPP with GPS-only, the products of WHU had the best performance on a time scale of 24 h, with the final position errors of 1.0 cm in the horizontal and vertical directions. The improvement in positioning accuracy with the multi-GNSS combination for different real-time products was not more than 17.1%. In the case of kinematic PPP for GPS-only, the products of WHU and ESA had the best performance on a time scale of 1 h, with the position errors of better than 10.8 cm and 9.5 cm in the horizontal and vertical directions, respectively. Compared with the results of GPS only, the improvement in positioning accuracy with the GREC combination for kinematic PPP was more significant and ranged from 49.4% to 72.8% in real-time mode. The results of CAS, DLR, GFZ and WHU for kinematic PPP on an hour scale with the GREC combination had positioning errors smaller than 5.2 cm.

Author Contributions: Conceptualization, C.Y. and Y.Z.; Methodology, C.Y. and K.X.; Software, C.Y. and Y.Z.; Validation, C.Y., Q.C. and K.X.; Writing—original draft, C.Y.; Writing—review and editing, C.Y. and J.C.; Visualization, C.Y.; Supervision, J.C. and B.W.; Funding acquisition, J.C. and B.W. All authors have read and agreed to the published version of the manuscript.

Funding: This research was funded by the Program of Shanghai Academic/Technology Research Leader (No.20XD1404500); the National Natural Science Foundation of China (No.11673050); the National Natural Science Foundation of China (No. 41904034); the Key Program of Special Development funds of Zhangjiang National Innovation Demonstration Zone (Grant No. ZJ2018-ZD-009); and the National Key R&D Program of China (No. 2018YFB0504300); and the Key R&D Program of Guangdong province (No. 2018B030325001).

Acknowledgments: The authors gratefully acknowledge the IGS Data Center of Wuhan University for providing multi-GNSS precise orbit and clock products. We also acknowledge Geoscience Australia for providing the real-time data streams.

Conflicts of Interest: The authors declare no conflict of interest.

References

1. Zumberge, J.F.; Heflin, M.B.; Jefferson, D.C.; Watkins, M.M.; Webb, F.H. Precise point positioning for the efficient and robust analysis of GPS data from large networks. *J. Geophys. Res. Solid Earth* **1997**, *102*, 5005–5017. [CrossRef]
2. Kouba, J.; Héroux, P. Precise point positioning using IGS orbit and clock products. *GPS Solut.* **2001**, *5*, 12–28. [CrossRef]
3. Ge, M.; Gendt, G.; Rothacher, M.; Shi, C.; Liu, J. Resolution of GPS carrier-phase ambiguities in Precise Point Positioning (PPP) with daily observations. *J. Geod.* **2008**, *82*, 389–399. [CrossRef]
4. Griffiths, J. Combined orbits and clocks from IGS second reprocessing. *J. Geod.* **2019**, *93*, 177–195. [CrossRef] [PubMed]
5. Geng, J.; Yang, S.; Guo, J. Assessing IGS GPS/Galileo/BDS-2/BDS-3 phase bias products with PRIDE PPP-AR. *Satell. Navig.* **2021**, *2*, 17. [CrossRef]
6. Agrotis, L.; Caissy, M.; Ruelke, A.; Fisher, S. Real-Time Service Technical Report 2014. In *IGS Technical Report 2014*; IGS Central Bureau: Pasadena, CA, USA, 2014; pp. 171–178.
7. Hadas, T.; Bosy, J. IGS RTS precise orbits and clocks verification and quality degradation over time. *GPS Solut.* **2015**, *19*, 93–105. [CrossRef]
8. Elsobeiey, M.; Al-Harbi, S. Performance of real-time Precise Point Positioning using IGS real-time service. *GPS Solut.* **2016**, *20*, 565–571. [CrossRef]
9. Chen, J.; Li, H.; Wu, B.; Zhang, Y.; Wang, J.; Hu, C. Performance of real-time precise point positioning. *Mar. Geod.* **2013**, *36*, 98–108. [CrossRef]
10. *RTCM 10403.3*; Differential GNSS (Global Navigation Satellite Systems) Services. RTCM: Arlington, TX, USA, 2016; Version 3, No. 104.
11. Weber, G.; Mervart, L.; Lukes, Z.; Rocken, C.; Dousa, J. Real-time clock and orbit corrections for improved point positioning via NTRIP. In Proceedings of the ION GNSS 20th International Technical Meeting of the Satellite Division, Fort Worth, TX, USA, 25–28 September 2007.
12. Wang, Z.; Li, Z.; Wang, L.; Wang, X.; Yuan, H. Assessment of Multiple GNSS Real-Time SSR Products from Different Analysis Centers. *ISPRS Int. J. Geo-Inf.* **2018**, *7*, 85. [CrossRef]
13. Wang, L.; Li, Z.; Ge, M.; Neitzel, F.; Wang, Z.; Yuan, H. Validation and Assessment of Multi-GNSS Real-Time Precise Point Positioning in Simulated Kinematic Mode Using IGS Real-Time Service. *Remote Sens.* **2018**, *10*, 337. [CrossRef]
14. Montenbruck, O.; Steigenberger, P.; Prange, L.; Deng, Z.; Zhao, Q.; Perosanz, F.; Romero, I.; Noll, C.; Stürze, A.; Weber, G.; et al. The Multi-GNSS Experiment (MGEX) of the International GNSS Service (IGS)—Achievements, prospects and challenges. *Adv. Space Res.* **2017**, *59*, 1671–1697. [CrossRef]
15. Li, X.; Ge, M.; Zhang, H.; Nischan, T.; Wickert, J. The GFZ Real-Time GNSS Precise Positioning Service System and Its Adaption for COMPASS. *Adv. Space Res.* **2013**, *51*, 1008–1018. [CrossRef]
16. Rülke, A.; Agrotis, L. IGS Realtime Service Technical Report 2016. In *IGS Technical Report 2016*; IGS Central Bureau: Pasadena, CA, USA, 2016; p. 179.
17. Hauschild, A.; Montenbruck, O. Kalman-filter-based GPS clock estimation for near real-time positioning. *GPS Solut.* **2009**, *13*, 173–182. [CrossRef]
18. Abdi, N.; Ardalan, A.A.; Karimi, R.; Rezvani, M.-H. Performance Assessment of Multi-GNSS Real-Time PPP over Iran. *Adv. Space Res.* **2017**, *59*, 2870–2879. [CrossRef]
19. Chen, L.; Zhao, Q.; Hu, Z.; Jiang, X.; Geng, C.; Ge, M.; Shi, C. GNSS Global Real-Time Augmentation Positioning: Real-Time Precise Satellite Clock Estimation, Prototype System Construction and Performance Analysis. *Adv. Space Res.* **2018**, *61*, 367–384. [CrossRef]
20. Zhang, L.; Yang, H.; Gao, Y.; Yao, Y.; Xu, C. Evaluation and Analysis of Real-Time Precise Orbits and Clocks Products from Different IGS Analysis Centers. *Adv. Space Res.* **2018**, *61*, 2942–2954. [CrossRef]

21. Wang, A.; Zhang, Y.; Chen, J.; Wang, H. Improving the (re-)convergence of multi-GNSS real-time precise point positioning through regional between-satellite single-differenced ionospheric augmentation. *GPS Solut.* **2022**, *26*, 39. [CrossRef]
22. Yan, C.; Wang, Q.; Zhang, Y.; Ke, F.; Gao, W.; Yang, Y. Analysis of GNSS Clock Prediction Performance with Different Interrupt Intervals and Application to Real-Time Kinematic Precise Point Positioning. *Adv. Space Res.* **2020**, *65*, 978–996. [CrossRef]
23. Xiao, X.; Shen, F.; Lu, X.; Shen, P.; Ge, Y. Performance of BDS-2/3, GPS, and Galileo Time Transfer with Real-Time Single-Frequency Precise Point Positioning. *Remote Sens.* **2021**, *13*, 4192. [CrossRef]
24. Lu, C.; Chen, X.; Liu, G.; Dick, G.; Wickert, J.; Jiang, X.; Zheng, K.; Schuh, H. Real-Time Tropospheric Delays Retrieved from Multi-GNSS Observations and IGS Real-Time Product Streams. *Remote Sens.* **2017**, *9*, 1317. [CrossRef]
25. Kazmierski, K.; Sośnica, K.; Hadas, T. Quality Assessment of Multi-GNSS Orbits and Clocks for Real-Time Precise Point Positioning. *GPS Solut.* **2018**, *22*, 11. [CrossRef]
26. Liu, T.; Jiang, W.; Laurichesse, D.; Chen, H.; Liu, X.; Wang, J. Assessing GPS/Galileo Real-Time Precise Point Positioning with Ambiguity Resolution Based on Phase Biases from CNES. *Adv. Space Res.* **2020**, *66*, 810–825. [CrossRef]
27. Li, B.; Ge, H.; Bu, Y.; Zheng, Y.; Yuan, L. Comprehensive Assessment of Real-Time Precise Products from IGS Analysis Centers. *Satell. Navig.* **2022**, *3*, 12. [CrossRef]
28. IGS RTWG. IGS State Space Representation (SSR) Format Version 1.00. 2020. Available online: https://files.igs.org/pub/data/format/igs_ssr_v1.pdf (accessed on 10 October 2022).
29. Stürze, A.; Mervart, L.; Weber, G.; Rülke, A.; Wiesensarter, E.; Neumaier, P. The New Version 2.12 of BKG Ntrip Client (BNC). In Proceedings of the EGU General Assembly 2016, Vienna, Austria, 17–22 April 2016; Volume 18, p. 12012.
30. Li, X.; Pan, L. Precise Point Positioning with Almost Fully Deployed BDS-3, BDS-2, GPS, GLONASS, Galileo and QZSS Using Precise Products from Different Analysis Centers. *Remote Sens.* **2021**, *13*, 3905. [CrossRef]
31. Wang, A.; Chen, J.; Zhang, Y.; Meng, L.; Wang, B.; Wang, J. Evaluating the impact of CNES real-time ionospheric products on multi-GNSS single-frequency positioning using the IGS real-time service. *Adv. Space Res.* **2020**, *66*, 2516–2527. [CrossRef]
32. Zhang, Y.; Chen, J.; Gong, X.; Chen, Q. The Update of BDS-2 TGD and Its Impact on Positioning. *Adv. Space Res.* **2020**, *65*, 2645–2661. [CrossRef]
33. Böhm, J.; Möller, G.; Schindelegger, M.; Pain, G.; Weber, R. Development of an Improved Empirical Model for Slant Delays in the Troposphere (GPT2w). *GPS Solut.* **2015**, *19*, 433–441. [CrossRef]
34. Zhou, F.; Dong, D.; Li, P.; Li, X.; Schuh, H. Influence of Stochastic Modeling for Inter-System Biases on Multi-GNSS Undifferenced and Uncombined Precise Point Positioning. *GPS Solut.* **2019**, *23*, 59. [CrossRef]
35. Allende-Alba, G.; Montenbruck, O.; Hackel, S.; Tossaint, M. Relative Positioning of Formation-Flying Spacecraft Using Single-Receiver GPS Carrier Phase Ambiguity Fixing. *GPS Solut.* **2018**, *22*, 68. [CrossRef]